Available online at www.sciencedirect.com
ScienceDirect
Molecular & Biochemical Parasitology 156 (2007) 175–190
MOLECULAR & BIOCHEMICAL PARASITOLOGY

# Dileucine signal-dependent and AP-1-independent targeting of a lysosomal glycoprotein in *Trypanosoma brucei*

Clare L. Allen [a], Dangjin Liao [a,b], Wei-Lian Chung [a], Mark C. Field [a,*]

[a] *The Molteno Building, Department of Pathology, Tennis Court Road, University of Cambridge, Cambridge CB2 1QP, UK*
[b] *Sichuan Academy of Animal Science, 7 Niu Sha Road, Chengdu 610066, Sichuan, PR China*

Received 8 May 2007; received in revised form 26 July 2007; accepted 30 July 2007
Available online 6 August 2007

**Abstract**

Sorting of *trans*-membrane proteins destined for the lysosome is achieved by selective inclusion into post-Golgi transport vesicles. In higher eukaryotes sorting may be mediated by a peptidic motif, principally acidic clusters and tyrosine- or dileucine-based cytoplasmic signals or by inclusion of mannose-6-phosphate (M6P) into the N-glycans of lysosomal proteins. In African trypanosomes a major lysosomal *trans*-membrane protein is CB-1/p67. The cytoplasmic domain of p67 lacks tyrosine and lysine, but does contain a canonical dileucine sequence embedded within an acidic region. AP-1, -3 and -4 adaptin complexes, which recognise tyrosine- and dileucine-sorting signals, are encoded by the trypanosome genome, but the genes for M6P-receptors or activities required to produce M6P are absent, suggesting that lysosomal delivery of p67 is most likely adaptin-mediated. By construction of p67 reporter constructs we show that the dileucine signal is necessary and sufficient for efficient lysosomal delivery of a *trans*-membrane protein in bloodstream stage trypanosomes. However, this targeting does not require AP-1, as knockdown of the trypanosome γ-adaptin subunit by RNAi has no detectable effect on the location or maturation of p67. These data suggest that p67 is targeted to the lysosome by dileucine-dependent but AP-1-independent mechanisms.


*Keywords:* Trypanosome; Protein transport; Vesicle trafficking; Endocytosis; Adaptor complex

## 1. Introduction

Lysosomal targeting of biosynthetic polypeptides in higher eukaryotes is principally mediated *via* post-Golgi sorting processes. The AP adaptin complexes are responsible for recognition of protein cargo molecules *via* direct binding to short specific sequence motifs (reviewed in [40]). The adaptor complexes AP-1 to -4 are conserved throughout the eukaryotic lineage [1] and contain two heavy chains (one representative of the closely related β-family and a second designated α, γ, δ or ε), a medium μ chain and a small σ chain. The AP complexes recognise primarily tyrosine, NPXY/YXXØ, and dileucine, [DE]XXXL[LI], based signals in cargo molecules; the μ chain appears important in recognition of polypeptide-based sorting signals, while additional interactions serve to integrate the adaptors into coat systems [2]. In higher eukaryotes AP-1 and -2 interact with clathrin and mediate transport from the *trans*-Golgi network/endosome and plasma membrane, respectively, while AP-3 and -4 function in *trans*-Golgi network and endosomal trafficking [40]. Additional complexes, including Dab2, stonin, PACS-1 and GGA are specific to animals and yeasts and may also recognise DXXLL-based signals [1,3,40]. A further lysosomal targeting mechanism is the addition of mannose-6-phosphate (M6P) to the N-glycans of soluble proteins, principally lysosomal hydrolases; this can be effectively ruled out for trypanosomatids due to the absence of the relevant open reading frames from the trypanosome genome.

Predominant metazoan lysosomal *trans*-membrane proteins are the LAMP glycoproteins. LAMPs are extensively *N*-glycosylated type I membrane proteins with comparatively short cytoplasmic domains and are proposed to provide a mainly

*Abbreviations:* BSA, bovine serum albumin; BSF, bloodstream form; DAPI, 4′-6-diamidino-2-phenylindole; GGA, γ-adaptin Golgi associated; GPI, glycosylphosphatidylinositol; IFA, indirect fluorescence analysis; M6P, mannose-6-phosphate; ORF, open reading frame; (v)PBS, (Voorheis's modified) phosphate-buffered saline; PCF, procyclic culture form; RNAi, RNA interference; TGN, *trans*-Golgi network; VSG, variant surface glycoprotein

* Corresponding author. Tel.: +44 1223 333734.
*E-mail address:* mcf34@cam.ac.uk (M.C. Field).

0166-6851/$ – see front matter © 2007 Elsevier B.V. All rights reserved.
doi:10.1016/j.molbiopara.2007.07.020

protective function, preventing autolytic lysosomal membrane degradation, although a direct role in lysosomal biogenesis is also suspected [4]. LAMPs are delivered to the lysosome *via* a tyrosine-based signal, which is strongly suggestive of at least partial routing *via* the plasma membrane [40] and AP-3 knockouts can disrupt targeting of LAMP glycoproteins [5]. By contrast, the M6P-receptor, which also has a tyrosine-based targeting signal, is sorted *via* AP-1 [6].

*Trypanosoma brucei* is evolutionarily distant from the major model organisms [42]. The major lysosomal glycoprotein in trypansomatids is p67 [38] and while the function is unknown the p67 polypeptide has a similar topology to LAMPs and is extensively *N*-glycosylated [7]. Extensive proteolytic processing accompanies p67 maturation, reflecting extensive peptidase activity residing within the endosomal system [17]. In mammalian stages p67 likely progresses to the lysosome *via* post-Golgi sorting, but some evidence suggests an indirect route operates involving initial export to the cell surface [7]. p67 contains a [E/D]EDELL dileucine sequence within an acidic short cytoplasmic domain, but lacks tyrosine or lysine residues; the latter excluding ubiquitylation as a mechanism. Removal of the cytoplasmic domain prevents lysosomal targeting of p67 [17] but this mutation may have several effects on the resulting behavior of the truncated protein.

The *T. brucei* cell surface is dominated by molecules bearing a glycosylphosphatidylinositol (GPI)-anchor, and maintenance of surface composition is required for cell cycle progression in the mammalian form [8]. Pathways for plasma membrane component trafficking have likely evolved to facilitate maintenance of the surface structure. Internalisation is exclusively clathrin-mediated [9,26] and components are returned to the surface *via* a highly active recycling system [10,26]. Specific secondary loss of the AP-2 adaptor complex from *T. brucei* has been reported [11,12], together with an absence of Dab2, GGAs, PACS-1 and stonins [1]. Therefore the adaptor complement in trypanosomes is likely simpler than in higher eukaryotes. AP-1 in the procyclic form has been implicated in trafficking of CRAM from *in vitro* interaction data [13], but the overall impact of AP-1 on transport is not known. Here we examine the role of AP-1 and the dileucine cytoplasmic motif of p67 in lysosomal targeting in *T. brucei*.

## 2. Materials and methods

### 2.1. Cell culture

Bloodstream form (BSF) and procyclic form (PCF) *T. brucei* Lister 427 cells were maintained in HMI-9 and SDM-79 media, respectively, supplemented with 10% tetracycline-free foetal bovine serum (Autogen Bioclear) as described previously [9]. To maintain tetracycline responsiveness the tetracycline-inducible cell lines BSF 90-13 and PCF 29-13 were cultured in the continual presence of 2 $\mu g\,ml^{-1}$ G418 and 1 $\mu g\,ml^{-1}$ phleomycin (BSFs) or 25 $\mu g\,ml^{-1}$ G418 and 1 $\mu g\,ml^{-1}$ phleomycin (PCFs). For growth curves, triplicate cultures were initiated at $5 \times 10^4$ cells $ml^{-1}$ (BSFs) or $1 \times 10^5$ cells $ml^{-1}$ (PCFs) and maintained within the logarithmic growth range. Cell concentration was determined using a Z2 Coulter counter (Beckman). Following transfection, expression of double-stranded RNA was induced by the addition of 1 $\mu g\,ml^{-1}$ tetracycline.

### 2.2. RNAi plasmid construction and transfection

To generate the RNAi plasmid p2T7$^{Ti}$β1Ad, a 495bp fragment of the Tbβ1Ad gene was PCR amplified from *T. brucei* genomic DNA using the primers 5′-AAGCTTCTGGGCACTCTAATCTCG-3′ and 5′-GGATCCCAGTGACGAAGCCGTAGG-3′, which contain the restriction sites for Hind III and BamHI, respectively, and inserted into the tetracycline inducible RNAi vector p2T7$^{Ti}$ [14]. This region was selected with the RNAit algorithm [15] to minimise the likelihood of off-target effects in the RNAi. A 526bp fragment of the Tbγ Ad gene was also PCR amplified from the same genomic DNA, using the primers 5′-CATCTCGAGTGCGCCTCCTAGTGCCCG-3′ and 5′-GGGAAGCTTGTGGTGTGGTTTGCG-3′, which contain the restriction sites for XhoI and Hind III, respectively. To insert this DNA fragment into the p2T7$^{Ti}$ vector, it was subcloned into pPCR-Script (Stratagene) and then excised using the XhoI site at the 5′ end of the fragment and the BamHI site in the multiple cloning site of the vector. The resulting 537bp XhoI–BamHI fragment was inserted into p2T7$^{Ti}$ to generate the RNAi plasmid p2T7$^{Ti}$γAd. Both of these RNAi constructs were transfected into PCF 29-13 and BSF 90-13 cell lines as previously described [9].

### 2.3. Antibody production

Tbγ Ad antisera were generated against an expressed protein fragment (residues 376–571) amplified from *T. brucei* genomic DNA using high fidelity Herculase DNA polymerase (Stratagene) with the following primers: 5′-GATGGATCCGAGACGAACGTGCGCCTC-3′ and 5′-AGCGAATTCGGGAACGACTCCAAGATG-3′. The PCR product was digested with BamHI and EcoRI and inserted into the expression vector pGEX-2TK (Amersham Biosciences). Polyclonal rabbit antibodies were raised against Tbγ Ad-GST recombinant fusion protein, which was SDS polyacrylamide gel purified due to insolubility when expressed in *Escherichia coli*, mixed with RIBI adjuvant (Sigma) and used to immunize rabbits on at least four immunizations spread over a period of 5 months. At least 0.5 mg of recombinant protein was used per immunization course. The resulting antibodies could not be affinity purified due to the insolubility of the recombinant GST fusion protein. All subsequent assays were therefore performed using the antiserum raised against the fusion protein.

### 2.4. Production of p67/BiPN reporter constructs and site-directed mutagenesis

Full length p67 together with 279bp and 216bp fragments corresponding to the extreme C-terminus of p67 (for constructs BiPNp67L and BiPNp67S, respectively) were amplified by PCR from *T. brucei* genomic DNA using the following

primers (enzymes in parenthesis); p67; 5′-ACGAAGCTTATGATGTGTACCGCAACCGTTA-3′ and 5′-AGGGGGCCCGTTCTGAGGATCTATAAGACCTT-3′ (HindIII and ApaI), BiPNp67L; 5′-ACGGCTAGCACCGATAATCAACCACCGTTTC-3′ and 5′-ACGGAATTCCTAGTTCTGAGGATCTATAAGACC-3′ (NheI and EcoRI) and BiPNp67S; 5′-ACGGCTAGCACCGATAATCAACCACCGTTTC-3′ and 5′-ACGGCTAGCGGGTTGCTGAAATTGTATAACTTT-3′ (NheI and EcoRI). Fragments were inserted into the pXS5$^{HA}$ or pXS5BiPN$^{HA}$ vectors to produce pXS5p67HA, pXS5BiPNp67L and pXS5BiPNp67S, respectively.

To generate DELL double point mutations (to AALL and DEAA) within the C-terminal sequence of p67, BiPNp67L or BiPNp67S, PCR was performed to amplify the p67 gene from *T. brucei* genomic DNA using the following primers; p67; DELL to AALL; 5′-ACGAAGCTTATGATGTGTACCGCAACCGTTA-3′ and AGGGGGCCCGTTCTGAGGATCTATAAGACCTTCAGCCTCTTCGGGAAGAAGAGCAGCCTC-3′ (HindIII and ApaI) and DELL to DEAA; 5′-ACGAAGCTTATGATGTGTACCGCAACCGTTA-3′ and 5′-AGGGGGCCCGTTCTGAGGATCTATAAGACCTTCAGCCTCTTCGGGAGCAGCTTCATCCTC-3′ (HindIII and ApaI), BiPNp67L; DELL to AALL; 5′-ACGGCTAGCACCGATAATCAACCACCGTTTC-3′ and ACGGAATTCCTAGTTCTGAGGATCTATAAGACCTTCAGCCTCCTTCGGGAAGAAG*AGCAGC*CTCTTC-3′ (NheI and EcoRI) and DELL to DEAA; 5′-ACGGCTAGCACCGATAATCAACCACCGTTTC-3′ and 5′-ACGGAATTCCTAGTTCTGAGGATCTATAAGACCTTCAGCCTCTTCGGG*AGCAGC*TTCATCCTC-3′ (NheI and EcoRI), BiPNp67S; DELL to AALL; 5′-ACGGCTAGCGGGTTGCTGAAATTGTATAACTTT-3′ and ACGGAATTCCTAGTTCTGAGGATCTATAAGACCTTCAGCCTCCTTCGGGAAGAAG*AGCAGC*CTCTTC-3′ (NheI and EcoRI) and DELL to DEAA; 5′-ACGGCTAGCGGGTTGCTGAAATTGTATAACTTT-3′ and 5′-ACGGAATTCCTAGTTCTGAGGATCTATAAGACCTTCAGCCTCTTCGGG*AGCAGC*TTCATCCTC-3′ (NheI and EcoRI). Products were inserted into pXS5BiPN$^{HA}$ or pXS5$^{HA}$ as above. All constructs and double point mutations were verified by restriction analysis and sequencing.

### 2.5. Protein electrophoresis and Western blotting

Protein samples were extracted from cells and separated by electrophoresis on 10% SDS-polyacrylamide gels, transferred to Hybond-ECL nitrocellulose membrane (Amersham Biosciences) and the membranes processed as previously described [9]. Primary antibodies were used at the following dilutions in Western blots: rabbit anti-TbγAd and rabbit anti-TbδAd were both used at 1:1000 to probe wild type parasite lysates and 1:250 to probe RNAi parasite lysates; rabbit anti-TbBiP, mouse anti-p67 (both from James Bangs) and mouse anti-TbαTub mAb (from Keith Gull) were both used at 1:5000. A commercial rabbit anti-HA9 (Santa Cruz Biotechnology) was used at 1:10,000. Incubations with commercial secondary anti-IgG rabbit or anti-IgG mouse horseradish peroxidase conjugates (Sigma) were performed at 10,000-fold dilution in TBST-milk.

### 2.6. Immunofluorescence microscopy

Indirect immunofluorescence microscopy was performed on BSF and PCF trypomastigotes harvested at log phase growth. BSF cells were washed in vPBS (136.9 mM NaCl, 3 mM KCl, 16 mM $Na_2HPO_4$, 3 mM $KH_2PO_4$, 45.9 mM sucrose, 10 mM glucose) then fixed for 1 h at 4 °C in 4% paraformaldehyde. Fixed cells were adhered to poly-L-lysine coated polyprep slides (Sigma) for 20 min at room temperature, then permeabilised with 0.1% Triton-X 100 (Sigma) in PBS for 10 min. Slides were blocked with 10% goat serum in PBS then incubated with the primary antibody at the appropriate dilution in blocking buffer at room temperature for a further hour. Unbound primary antibody was washed off with PBS/0.05% Triton-X 100 prior to incubation for 1 h at room temperature with secondary antibodies; Texas Red-conjugated goat anti-rabbit IgG or Oregon-Green labelled goat anti-mouse IgG (Molecular Probes), diluted according to manufacturer's instructions. Slides were washed and stained with DAPI (present in the mounting buffer at 0.5 μg ml$^{-1}$) to visualise the nucleus and kinetoplast. Essentially the same procedure was used for immunofluorescence microscopy of PCF trypomastigotes, except that these cells were fixed in 4% paraformaldehyde for 30 min at room temperature prior to adhesion to the slides. Cells were examined using a Nikon Eclipse E600 microscope and images were captured using a Photometrics CoolSNAP FX camera. Digital images were captured and false coloured using MetaMorph 5.0 software (Universal Imaging Corporation). Primary antibodies were used at the following dilutions: rabbit anti-TbCLH [11], 1:500, rabbit anti-TbBiP [16], 1:1500, mouse anti-p67 mAb280 [17], 1:500 and rabbit anti-TbRAB1 [18], 1:100. Rabbit and mouse anti-HA9 epitope IgG (both from Santa Cruz Biotechnology) was used at 1:1000. To quantitate surface expression of p67 constructs, the p67HA cell lines were stained with anti-p67 antibody following the method above (which detects an externally disposed epitope), but omitting the permiabilisation step. The fluorescence intensity in at least 20 randomly selected cells of each strain was measured from MetaMorph images captured under non-saturating conditions and at identical exposures.

### 2.7. Electron microscopy

Transmission electron microscopy was performed as described previously [9].

### 2.8. VSG export assay

VSG export was monitored exactly as described [9]. Briefly, $5 \times 10^7$ mid-log phase BSFp2T7$^{Ti}$γAd cells grown in the presence or absence of 1 μg ml$^{-1}$ tetracycline for 16 h were washed once in labelling medium (Met/Cys free Dulbecco's Modified Eagle's medium (DMEM) (Sigma) supplemented with 10% dialysed fetal bovine serum and 25 mM Hepes (pH7)), centrifuged and resuspended in 1 ml labelling medium (±tetracycline) and incubated for 15 min at 37 °C. Cells were pulse labelled for

7 min at 37 °C with [$^{35}$S] labelled Pro-mix (Amersham Biosciences) at 200 μCi ml$^{-1}$, then chased for up to 1 h (37 °C, 5% $CO_2$) by diluting the cells 1:10 with complete HMI 9 (±tetracycline). 1 ml aliquots of cells were removed at intervals during the chase period and placed on ice. Following centrifugation the cell pellets were washed in 1 ml ice-cold PBS/BSA, resuspended in 920 μl of hypotonic lysis buffer, then incubated for 5 min on ice, followed by 10 min at 37 °C to enable endogenous GPI-phospholipase C (GPI-PLC) to convert susceptible membrane form VSG to soluble VSG. Centrifugation isolated soluble VSG in the supernatant of the lysates. The pellet fraction (containing membrane bound VSG) was washed with ice-cold hypotonic lysis buffer then resuspended in 1 ml ice-cold sample lysis buffer and incubated on ice for 25 min to lyse the membranes and release the VSG. NP-40 was added to the supernatant fraction to bring all of the samples into the same buffer. Lysates were cleared by centrifugation and the supernatants retained for VSG recovery by ConA binding. ConA-sepharose 4B (Sigma) was added to the supernatants in the presence of $MnCl_2$ and $CaCl_2$ to aid binding, and mixed at 4 °C for 1 h. The ConA-sepharose with bound glycoproteins were then washed with ConA wash buffer, after which they beads resuspended in SDS-PAGE sample buffer and resolved on 10% SDS-PAGE gels loaded at $1 \times 10^6$ cell equivalents per lane. To detect labeled VSG, stained gels were fixed then treated with En$^3$Hance (NEN Life Sciences), before exposure to X-ray film (Kodak). The VSG bands were quantitated, together with background subtraction (adjacent area from the same lane) using ImageJ software.

### 2.9. p67 processing assay

Processing of p67 was followed as described previously [19,20]. Briefly, BSFp2T7γ$^{Ti}$Ad cells grown in the presence or absence of 1 μg ml$^{-1}$ tetracycline for 16 h were harvested, washed twice in Met/Cys free DMEM (Sigma) and resuspended to a final concentration of $1 \times 10^8$ ml$^{-1}$ in the same medium supplemented with dialysed fetal bovine serum and incubated for 15 min at 37 °C. Cells were pulse labelled for 15 min at 37 °C by addition of [$^{35}$S]-labelled Pro-mix (Amersham Biosciences) at 200 μCi ml$^{-1}$ then chased by 1:10 dilution in complete HMI9 medium. 1 ml samples were withdrawn at 0 and 30 min, 1 h, 2 h and 4 h into the chase period and placed on ice. Cells were washed in PBS and then lysed in ice-cold radioimmune precipitation (RIPA) buffer [19,20]. The lysates were precleared by mixing with 10 μl of a 50:50 slurry of protein A-sepharose beads (Amersham Biosciences) in RIPA buffer for 1 h at 4 °C. The supernatants were then mixed with 10 μl of anti-p67 mAb280 coated protein-A sepharose beads for 1 h at 4 °C. After washing the beads twice with RIPA buffer, twice with high salt RIPA buffer (500 mM NaCl) and twice with TBS, the immunoprecipitates were resuspended in 50 μl of loading buffer and run on 12% SDS-PAGE gels. Fixed and stained gels were treated with En$^3$Hance (NEN Life Sciences), dried and exposed to X-ray film (Kodak). The intensity of metabolically labelled protein bands was quantified using ImageJ software.

## 3. Results

### 3.1. Targeting of p67 depends on the presence of a DELL motif in the cytoplasmic domain

The *T. brucei* genome encodes two near identical copies of the p67 protein (Fig. 1A). Both retain a canonical [D/E]XXXL[L/I] putative dileucine adaptin—interaction motif, also partially conserved in the *Trypanosoma cruzi* orthologue. A second degenerate dileucine motif is present C-terminal to the canonical signal. The cytosolic domains are acidic, with p*I*s of 2.7 for Tb927.5.1830 and 4.2 for Tb927.5.1810. Deletion of the entire cytoplasmic portion of p67 results in partial mistargeting of p67 in BSF trypanosomes, broadly consistent with a trafficking role for the cytoplasmic domain [17]. We generated a panel of p67 mutants and chimeras using sequence derived from Tb927.5.1810 (p67B) and based around BiPNHA [21], containing the *trans*-membrane and cytoplasmic domains of p67 together with a junction region from the p67 ectodomain (Fig. 1B). Replacement of the p67 ectodomain by BiPN has the advantage of eliminating both targeting information and protein–protein interactions; specifically this allows the criterion of sufficiency for the transplanted region to be addressed (discussed in [21]). All constructs were transfected into BSF trypanosomes and transformants were obtained expressing an HA-tagged polypeptide of the expected size (Fig. 2); at least two clones for each construct were analysed with essentially identical results in each case.

An HA-reactive band of apparent molecular weight ∼100 kDa was obtained for p67HA—some heterogeneity was also detected, likely due to processing of the extensive p67 N-glycans (Fig. 2A). Faint additional lower molecular weight bands were detected on overexposed blots and likely correspond to proteolysed fragments of p67 (data not shown) [17]. p67HA with point mutations within the DELL motif expressed at similar levels to the native p67HA sequence as a predominant immunoreactive band of ∼100 kDa (Fig. 2A). By immunofluorescence it was clear that the HA-tagged wild type version of p67HA was faithfully targeted to the lysosome as there was excellent colocalisation of p67 and HA in a perinuclear compartment (Fig. 2B). The absence of mislocalised HA or p67 immunoreactivity resulting from the transgene demonstrated that the HA tag did not interfere with targeting.

BiPNp67S and BiPNp67L were also expressed at the correct size, as demonstrated by Western blot (Fig. 2A). However, BiPNp67S was predominantly recovered as a lower molecular weight species (P; processed) rather than as full length (F). By contrast BiPNp67L was mainly expressed as the full-length product, with only a minor processed population. The predicted sizes of the processed forms are consistent with cleavage C-terminal to the HA epitope, presumably within the ectodomain derived from p67 and mimicking the processing described for p67 itself [17]. This difference in processing efficiency can be accounted for by the locations of the two constructs. Specifically, BiPNp67L was effectively retained in the ER, likely protecting the polypeptide from peptidases present in post-ER portions of the transport pathway [17]. BiPNp67S was targeted to the

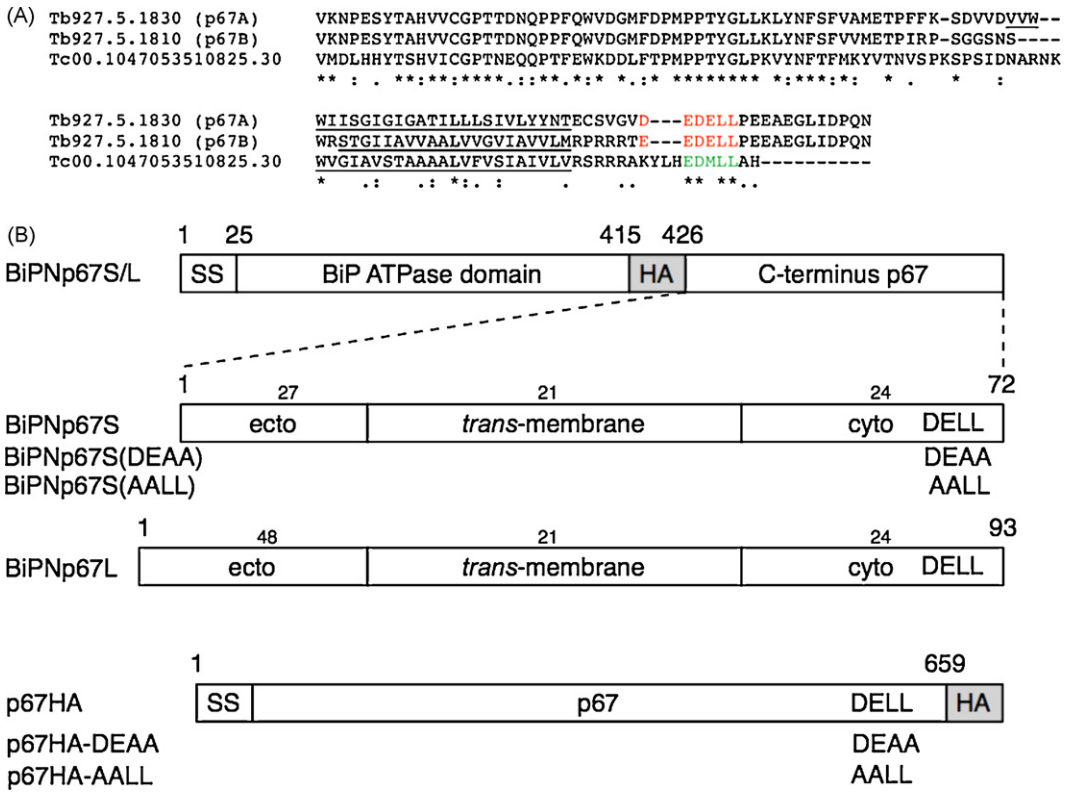


Fig. 1. AP-1 consensus interaction sequence in the cytoplasmic tail of p67. (Panel A) ClustalX alignment of the predicted amino acid sequences for the C-terminal region of the two p67 ORFs from *Trypanosoma brucei* (Tb927.5.1810/1830, p67A and p67B) together with the *Trypanosoma cruzi* orthologue. "⋆" indicates residues identical in all three sequences, ":" highly conserved, "." conserved, "-" gaps introduced into the alignment. The predicted position of the *trans*-membrane domain is underlined. The location of a sequence that conforms to the dileucine AP-1 consensus ([D/E]XXXL[L/I]) is also indicated in red in the *T. brucei* sequences and in green in the *T. cruzi* orthologue. (Panel B) Diagrammatic representation of p67-derived constructs used. p67HA is a full length version of p67 containing an HA-tag at the C-terminus; other constructs are based on BiPNHA [21] and contain the indicated regions of p67 derived from the C-terminal region of the ectodomain, the *trans*-membrane domain and the cytosolic domain. Mutagenesis was performed by mega-primer PCR and all constructs were contained within pXS5 [39]. Sequence numbering is based on Tb927.5.1810.

lysosome, accounting for processing of the protein in post-ER compartments. We propose that the ER location of BiPNp67L is likely due to misfolding, and hence ER retention, as part of the secretory pathway quality control system. Transfer of the p67 C-terminus to BiPN to create BiPNp67S, and the faithful targeting of that construct to the lysosome demonstrates sufficiency for this region for lysosomal delivery.

We examined if the EEDELL sequence was necessary by localisation of the two mutagenised versions of the construct, BiPNp67S-AALL and BiPNp67S-DEAA. In comparison to the respective wild type versions of the constructs, some targeting to the lysosome was retained but with considerably reduced efficiency, and with a prominent population of the HA-tagged protein at the cell surface (note that the HA epitope is positioned on the luminal/external side of the membrane) (Fig. 2B). We confirmed this result by analysis of the mutant forms of p67HA, with equivalent alterations to the DELL motif. These constructs appeared by immunofluorescence to be widely distributed across the cell surface, rather than exhibiting highly specific targeting to the lysosome, similar to the BiPNp67HA mutants (Fig. 2C). We probed for surface mislocalisation by analysis of cells by immunofluorescnce under conditions where internal antigens were not detected, i.e. without detergent permiabilisation, using antibody against p67, with a clear increase in surface p67 immunoreactivity in the mutated forms (Fig. 2C and D). Hence these data suggest that the presence of an intact DELL sequence is required for lysosomal targeting, and moreover that disruption of any one motif, i.e. DE or LL, is sufficient to interfere with targeting.

Taken together these observations indicate that the DELL sequence in p67 constitutes an authentic lysosomal targeting signal that is both necessary and sufficient for correct and efficient trafficking. Interestingly, mistargeting of BiPNp67S-AALL and p67HA-AALL suggests that the targeting signal in p67 may be more extensive than the canonical dileucine signal as defined in higher eukaryotes, and includes acidic residues N-terminal to the dileucine.

### 3.2. *Expression of AP-1 subunits in trypanosomes*

Adaptin complexes mediate the major dileucine-dependent transport pathways in higher eukaryotes. AP-1 components are constitutively expressed in trypanosomes, based both on Western analysis of the β-subunit and microarray transcritome analysis [11] (Koumandou and MCF, unpublished data), and interaction with CRAM, a type I membrane protein and the AP-1 μ subunit has been demonstrated *in vitro* [13]. AP-1 mediates a major trafficking pathway from the TGN to lysosomes

in higher eukaryotes, and disruption of AP-1 leads to mistargeting of many lysosomal proteins. Hence we selected AP-1 for analysis of potential function in p67 transport. We previously identified and described a β1-subunit, likely part of the AP-1 complex [11]. However, as β-subunits are closely related between complexes we selected a more specific AP-1 subunit sequence, the γ-subunit, for further investigation.

Antisera raised against the recombinant γ-subunit expressed in *E. coli* recognised a band of the predicted molecular weight (87.3 kDa) in lysates from both BSF and PCF stages of the parasite (Fig. 3A), indicating that, similar to the β1-subunit, the protein is expressed throughout the life cycle [11]. We used RNA interference (RNAi) to address AP-1 function (Fig. 3). In the bloodstream form RNAi of the β1- or γ-subunit resulted in cessation of growth following induction after 2 days, with a loss of cell viability in the cultures. Similar results were obtained in the insect stage, although as is common in RNAi, the kinetics were rather more extended such that the γ-subunit produced a significant growth defect by day 6 and the β1-subunit by day 7. The similarity of the RNAi effect on growth is consistent with β1- and γ-subunits comprising the same complex.

To confirm the specificity of the knockdown we analysed protein extracts of cells following induction of RNAi (Fig. 4). A clear loss of the γ-subunit was observed following induction in both bloodstream and procyclic forms (top and lower panels). Significantly, lysates of bloodstream stage cells that had been subjected to RNAi for the β1-subunit also demonstrated loss of the γ-subunit signal and in both life stages loss of the protein occurred with similar kinetics, so that <20% of the normal γ-subunit signal was obtained following 48 h induction (middle panel). The protracted appearance of a phenotype in the PCFs therefore suggests a lower requirement for AP-1 expression as the slower phenotype cannot be ascribed as less rapid turnover of the targeted gene product. Taken together this is further evidence that the β1- and γ-subunits form part of the same complex as evidence suggests that incompletely assembled complexes are unstable [22]. Unfortunately the γ-subunit antibody did not recognise specific compartments by immunofluorescence, despite repeated attempts and use of multiple fixation conditions (data not shown).

To confirm specific knockdown of the β1-subunit, which in contrast to the γ-subunit could not be assessed by Western analysis, we used semi-quantitative reverse transcriptase (RT)-PCR. To ensure that the PCR was performed under conditions sensitive to changes to mRNA levels we titred mRNA template concentration and cycle number (Fig. S1). A loss of specific product for the β1-subunit over a 24-h time period in the bloodstream form was obtained, whilst the α-tubulin control product was unchanged following RNAi for the β1-subunit. Neither product was generated when the RT step was omitted. These data confirm that the β1-subunit is specifically targeted by the β1-RNAi and therefore that the gene product is required for robust growth.

### 3.3. Adaptor AP-1 is required for maintenance of normal morphology and cell cycle progression

In order to analyse function and determine the kinetics of onset of a phenotype, we investigated the effect of AP-1 RNAi on progression though the cell cycle and on cellular morphology. Upon induction of γ-subunit RNAi we observed a slow increase in cells with abnormal morphology and also numbers of nuclei (Fig. 5A–C). Defects included the appearance of vesicular structures within the cytoplasm, rounding of the cells, and also enlargement of the flagellar pocket.

In BSFs, a gradual fall in the number of cells in interphase was observed (nucleus/kinetoplast content 1N:1K). This was initially

Fig. 2. A DELL sequence at the C-terminus of p67 is necessary and sufficient for lysosomal targeting in trypanosomes. (Panel A) Western blot analysis of total cell lysates from stable clones expressing various p67-derived constructs. Constructs were based on the Tb927.5.1810 sequence. All blots have been probed with mouse antibody to HA and are derived from $1 \times 10^6$ cell equivalents. (Top left panel) 427 parental trypanosome line and a clone expressing p67HA. Note the absence of immunoreactivity in the 427 line. p67HA migrates at the predicted molecular weight; heterogeneity can be accounted for by a combination of N-glycan and proteolytic processing. (Top right panel) Expression of p67HA mutants. Note the presence of a major band at ∼100 kDa in all lanes and similarity of expression levels. Data from representative clones is shown—similar data were obtained for at least two additional clones in each case. The blot has been exposed for a shorter time than the left hand panel to highlight the major band; more extensive processing, likely *N*-glycosylation, is seen for the p67HA-DEAA construct. (Lower left panel) Analysis of representative clones expressing BiPNp67S or BiPNp67L constructs. A contrast enhanced image of the gel between 45 and 65 kDa is shown below the main panel to highlight the presence of two bands in these lysates; F corresponds to the predicted migration position of the full length product and P to a processed form that is likely cleaved between the HA tag and the N-terminal side of the *trans*-membrane domain. (Lower right panel) BiPNp67S isoforms. Note that for each construct multiple clones were analysed and in all cases data obtained were essentially identical. (Panel B) Localisation of p67-derived constructs by immunofluorescence. (Top panels) p67HA is localised to the lysosome, as demonstrated by efficient colocalisation of HA and p67. Note that for the p67HA constructs both p67 and HA will be detected—the observation that essentially all HA is located in the lysosomal region and not elsewhere provides strong evidence for faithful targeting of the tagged construct, as mistargeting would result in partial alterations in both HA and p67 localisations. The C-terminal portion of p67 is sufficient for delivery as shown by transfer to BiPN to create BiPNp67S; again HA and p67 are colocalised. Inclusion of an additional 21 amino acids results in misfolding as the BiPBp67L construct is retained in the ER. (Lower panels) Mutagenesis of the DELL motif to either DEAA or AALL results in inefficient lysosomal targeting. Both BiPNp67SAALL and BiPNp67SDEAA are localised partly in the lysosome but substantially on the plasma membrane. In each panel the BiPN/p67 construct is localised by HA staining (red) and p67 is used to locate the lysosome (green). DNA is stained with DAPI. Images are representative and consistent staining was obtained for each clone. (Panel C) Surface expression of p67HA isoforms. Cells stably expressing one of the p67HA isoforms were stained with anti-p67 antibody (green) and anti-VSG antibody (red) in the absence of detergent to specifically detect surface fluorescence. Note that the expression levels of all three p67HA isoforms are similar (panel A). In cells expressing the wild type version of p67 essentially no fluorescence is detected, whilst for the mutants significant diffuse surface staining is detected, representing efficient targeting of the ectopic gene product and consistent with the data in panel B. Scale bar = 2 μm. Note that the signal for p67 has been enhanced as the antigen is significantly less abundant that VSG, but this is equivalent for all panels. (Panel D) Quantitation of surface fluorescence for p67HA mutants. A very significant increase in fluorescence is detected in the two p67HA mutant cell lines ($p > 0.0001$), consistent with a loss of targeting efficiency. Data are shown in relative fluorescence, with the mean and standard deviations given; "*n*=" refers to the number of individual cells examined. S and L correspond to short and long junction forms of BiPNp67, respectively.

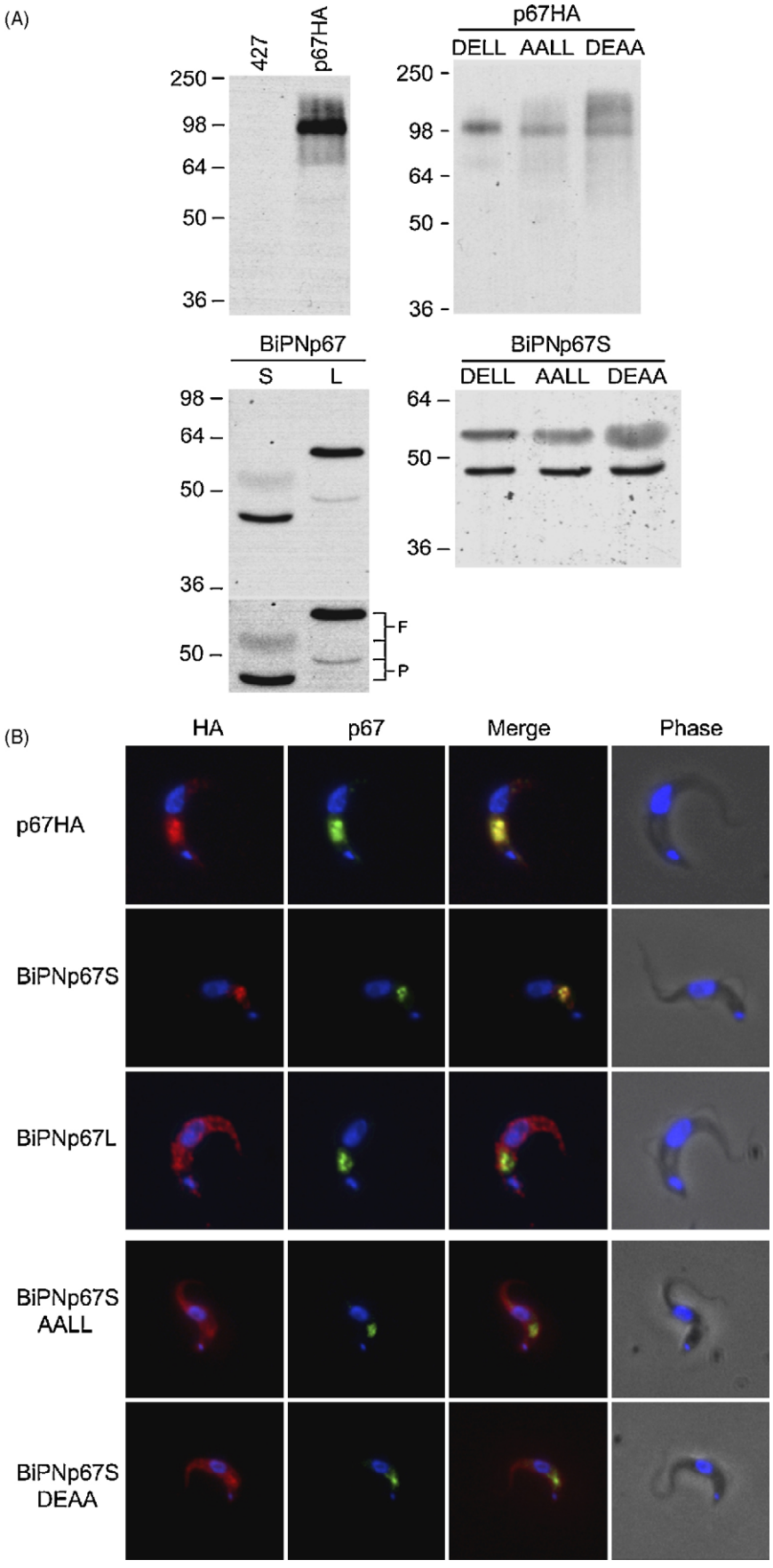


Fig. 2. (*Continued*).

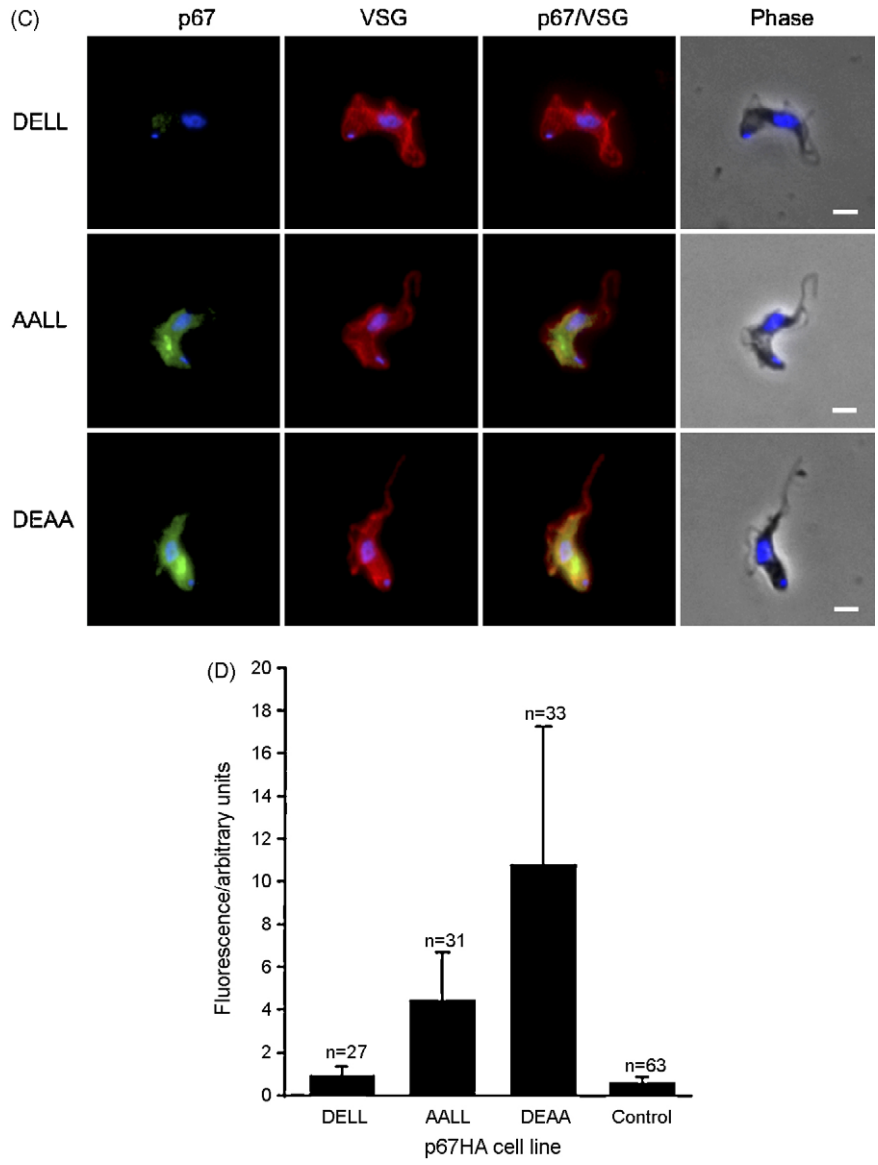


Fig. 2. (*Continued*).

due to an increase in 2N:2K cells, but at later times the 2N:2K incidence returned to normal levels with an increase in multinucleated cells (>2N:2K) (Fig. 5D, left). We also observed cells with enlarged nuclei at later time points, indicating that not only was there a defect in cytokinesis, seen as an increase in 2N:2K and >2N:2K cells, but also nuclear division (Fig. 5D). The phenotype is also consistent with a defect to membrane traffic, either in delivery of membrane to the growing cytokinesis furrow or in the correct trafficking of critical components required for completion of cell division. A significant proportion of BSF cells recapitulated the enlarged flagellar pocket (BigEye) phenotype [9] suggesting an endocytosis defect (Fig. 5E). However, the proportion of cells with this feature was minor (≤20%) and onset was comparatively slow, and emergence of the enlarged pocket is likely a manifestation of general disruption to membrane transport, which ultimately affects endocytic activity. Ultrastructural analysis also demonstrated defects within the endomembrane system, principally the accumulation of electron dense structures in the cytoplasm, an enlarged, crenelated flagellar pocket (Fig. 6F–H) similar to Rab5 RNAi [20] and also prominent multivesicular bodies (MVBs). The structure with electron dense deposits at the membrane and the presence of prominent MVBs is similar to a phenotype observed by Williams et al. in starved or cysteine peptidase knockout *Leishmania* promastigotes, and interpreted as part of the autophagic pathway [23], consistent with a defect in endosomal trafficking being induced by the γ-subunit knockdown. Hence a pleotropic defect in morphology and mitosis is obtained by ablation of AP-1 and suggests that AP-1 mediates an important trafficking pathway in BSF trypanosomes.

In procyclics a less pronounced morphological defect occurred following knockdown of the γ-subunit. Cells became rounded with a clear accumulation of numerous phase-light vesicles as observed by phase contrast (Fig. 5C). A small decrease in the incidence of interphase cells likely reflects the growth defect in these cells (Fig. 5D), but a prominent block to cell

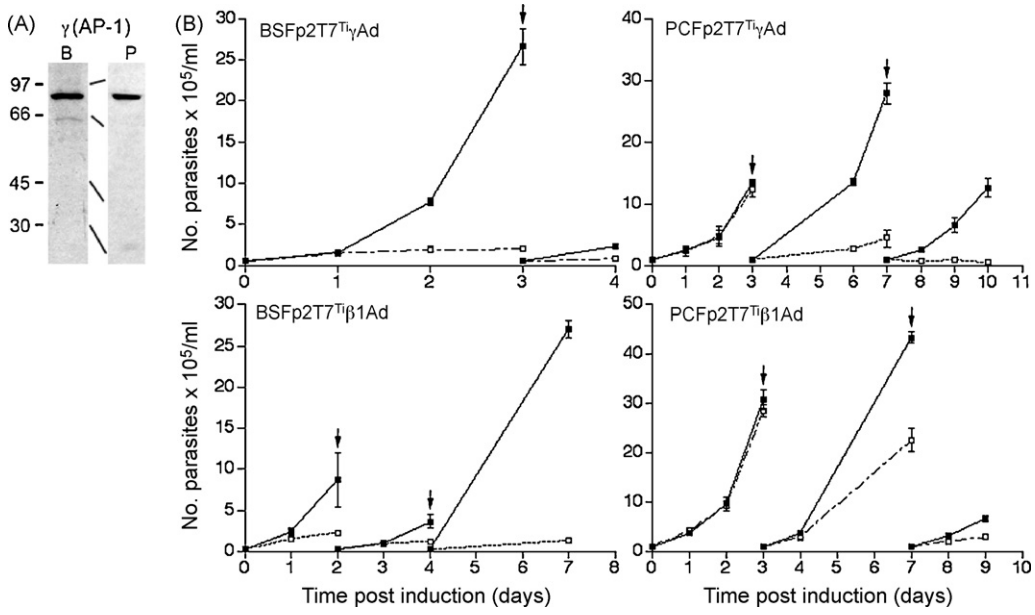


Fig. 3. The AP-1 complex of *T. brucei* is constitutively expressed and essential. (Panel A) Western blot analysis of whole cell lysates from bloodstream (B) and procyclic (P) ($1 \times 10^7$ cell equivalents) immunoprobed with rabbit antisera raised against recombinant adaptin subunit TbγAd. A single band of the expected molecular weight is found with equal intensity in both life stages. The scale to the left of each lane represents relative molecular mass in kDa. Expression analysis of the Tbβ1Ad subunit has been previously described [11]. (Panel B) Growth curves for bloodstream (BSF) and procyclic (PCF) form trypanosomes transformed with the $p2T7^{Ti}$ RNAi constructs for TbγAd and Tbβ1Ad. Cells were grown in the presence (open squares) or absence (closed squares) of 1 μg ml$^{-1}$ tetracycline. Induction was initiated at time zero. Cell number was determined by coulter counter at the indicated times. Cells were maintained under logarithmic growth conditions by periodic dilution (indicated by arrows and breaks in the growth curves). Each data point represents the mean of triplicate cultures (±standard deviation). The data are representative of multiple experiments.

cycle progression was not observed. In induced cells the most prominent ultrastructural defects were accumulation of vesicles within the cytoplasm, which probably correspond to those seen in the light microscope (Fig. 5C), and also rather large vacuoles (>0.2 mM diameter) with electron dense material on the limiting membrane. The origin of the large vacuole is not clear, but the accumulation of the small vesicular structures is consistent with a defect in post-Golgi transport, and is similar to that observed by RNAi knockdown in PCFs for clathrin [9]. However, in contrast to the PCF CLH RNAi phenotype where the Golgi becomes enlarged and distorted, the Golgi complex itself appears unaffected in these cells (Fig. 6). Hence in the procyclic form a comparatively minor and late onset phenotype is observed, suggesting that AP-1 does not mediate a major trafficking route in insect form trypanosomes.

### *3.4. AP-1 is not required for efficient trafficking of p67 or exocytosis of VSG*

To specifically analyse trafficking of p67 we used the assay described by Alexander et al. [17] and used by us to demonstrate trafficking defects associated with knockdown of Rab4 [19,20]. p67 is synthesized as a 100 kDa precursor protein in the endoplasmic reticulum, is matured to a 150 kDa form in the Golgi complex by elaboration of its N-glycans, and is then subject to proteolysis generating first a 72 kDa form and subsequently 42 and 32 kDa species as a late endosomal/lysosomal event; an example is shown in Fig. 7A. Unexpectedly, we observed that formation and disappearance of all five characterised forms of p67 were essentially unaltered by loss of the AP-1 γ-subunit after 18 h induction (this time point chosen as a compromise between loss of expression of the γ-subunit and the emergence of grossly altered morphology at ∼24 h) (Fig. 7A). Hence these data suggest that p67 delivery to the lysosome is largely independent of AP-1 expression.

We also monitored export of newly synthesised VSG as a marker for exocytosis and a validated assay previously used by us to investigate the effect of RNAi on VSG transport [9,18,24,25]. Again, no defect in the kinetics of delivery of VSG to the cell surface could be detected (Fig. 7B). Hence we were not able to detect a defect in progress through the ER, Golgi complex, delivery to the lysosome or alterations in the kinetics of N-glycan elaboration.

### *3.5. AP-1 knockdown does not alter localisation of p67*

We chose to confirm the absence of a clear effect of AP-1 knockdown on p67 trafficking by immunofluorescence. We selected several membrane vesicle markers for our analysis; BiP for the ER [16], clathrin for endosomes [9,11,26] and Rab1 for the Golgi complex [18]. We performed the analysis on aliquots of cultures induced for the AP-1 γ-subunit for various times, and allowed the induction in the remaining cells in the culture to proceed until we obtained morphological defects, to demonstrate that the RNAi induction was effective.

In BSFs we saw the expected BiP reticular staining indicative of the ER (Fig. 8A) which was not perturbed significantly, and only became significantly abnormal after 24 h induction when

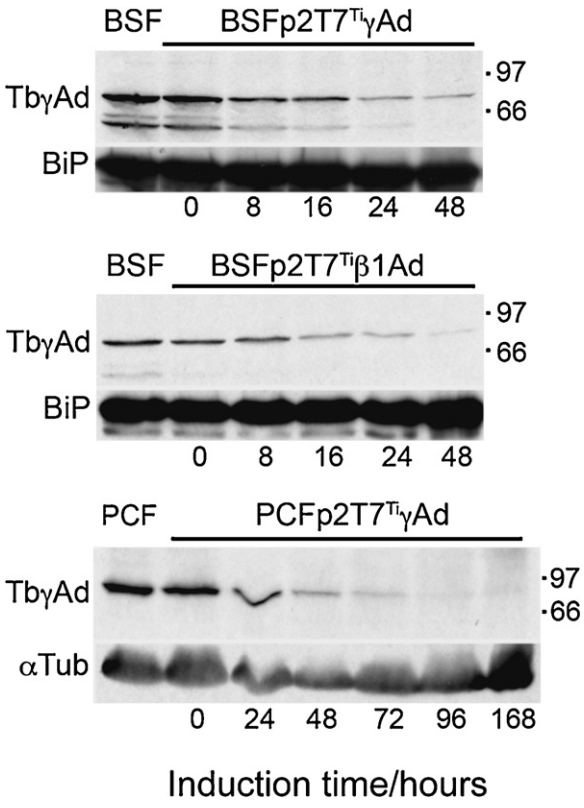


Fig. 4. Demonstration of association between TbγAd and Tbβ1Ad. Western blot analysis of TbγAd expression under RNAi induction. Aliquots of each culture were taken at the indicated times post-induction with 1 μg ml$^{-1}$ tetracycline, solubilised and proteins separated by SDS-PAGE for analysis by Western blot. The samples shown were taken from cultures of BSF (upper panel) or PCF (lower panel) cells transformed with p2T7$^{Ti}$ RNAi constructs for TbγAd or BSF cells transformed with the p2T7$^{Ti}$ RNAi construct for Tbβ1Ad (middle panel). The leftmost lane of each blot is a control lysate from parental cells. Blots were probed with anti-TbγAd antiserum, then stripped and re-probed with antibody against either the ER chaperone BiP or α-tubulin (αTub) as a loading control. The scale on the right of each blot represents relative molecular mass in kDa. Additional bands in the upper panel reflect proteolysis of TbγAd, as the data in Fig. 1 show the antisera to be monospecific.

cellular morphology was strongly altered, consistent with no role for AP-1 in maintaining ER structure. Surprisingly, clathrin location was also maintained even in the presence of significantly distorted cell morphologies as seen after 18 h. Staining became diffuse at 24 h, likely reflecting a general disorganisation of endosomal and post-Golgi membranes. This is broadly consistent with a role for AP-1 in post-Golgi transport and supported by the ultrastructural evidence, but argues against a specific role in endocytosis *per se*. Further, Rab1, which localises to the *cis*-face of the Golgi complex, was largely unaffected until the cells became severely distorted, again ruling out a major defect in ER to Golgi or intra-Golgi transport. Most significantly, p67 also retained lysosomal localisation and hence is targeted faithfully, with no clear evidence for accumulation at an earlier compartment within the lysosomal trafficking route. We cannot rule out a residual contribution to the immunofluorescence signal from p67 that had reached the lysosome prior to induction, but at 24 h we expect most p67 to have turned over. In PCFs BiP was clearly faithfully targeted even at 6 days post-induction, even when some abnormal morphologies were present within the culture. For Rab1, some delocalisation became apparent at 6 days – this may indicate that some of the accumulated vesicles contain Rab1, and would be consistent with a Golgi origin for some of these structures. By contrast p67 retained correct targeting during the period of knockdown. At later times some loss of signal was observed, but significantly the remaining signal was correctly located for most cells, suggesting the absence of a major defect in lysosomal targeting in the procyclic form. Hence knockdown of the adaptin γ-subunit did not elicit a potent block to lysosomal targeting of p67 in either life stage, suggesting that normal trafficking of the major lysosomal protein may proceed in the absence of full AP-1 expression.

## 4. Discussion

Our major findings concerning lysosomal targeting signals in p67 are as follows. Firstly, we demonstrate that p67 possesses a canonical dileucine signal within the cytoplasmic C-terminal domain that is essential for lysosomal targeting. Secondly, the cytoplasmic domain of p67 is sufficient for lysosomal targeting by virtue of transplantability with additional evidence based on BiPN-based chimeric constructs. Thirdly, we find a requirement for DE residues immediately N-terminal to the main lysosomal targeting dileucine motif—these residues appear to be a major determinant in that mutagenesis severely compromises targeting behavior of the p67 and BiPN chimeras. Fourthly, loss of efficient lysosomal targeting in p67 or BiPN chimeras results in surface expression, suggesting that this is the default pathway for *trans*-membrane glycoproteins in trypanosomes.

The presence of a functional dileucine motif in p67 suggests, by analogy with higher eukaryotes, engagement with either adaptor complexes or GGA proteins, but as trypanosomes lack GGA genes this latter possibility can be excluded [1]. Involvement of DE residues N-terminal to the dileucine motif is significant as these residues occupy positions that, in higher eukaryotes, are not especially important in specifying adaptor complex interactions, and may suggest either a second overlapping signal or that adaptin recognition is more extensive in trypanosomes. We note the presence of a second dileucine-related signal C-terminal to the DELL sequence investigated here—this signal is divergent from the canonical sequence, and while we cannot rule out a role in targeting, it is clear that the DELL signal is a major sorting determinant. Acidic clusters, without dileucines, occur in several proteins including furin, and which are important for both intracellular trafficking and endocytosis [27]. The presence of a secondary signal is consistent with the incomplete mislocalisation of the BiPNp67 mutants and the lack of mistargeting of p67 in the AP-1 RNAi cells, suggesting that an additional sorting system may operate. Signal divalency has been described recently for the G1 cyclin CLN3 [28].

The presence of a subpopulation of mutant p67 chimeras at the cell surface may suggest that p67 is at least partially trafficked *via* the indirect cell surface route. However, considerable experimental evidence is inconsistent with this model; specifically RNAi knockdown of TbCLH, the clathrin heavy chain

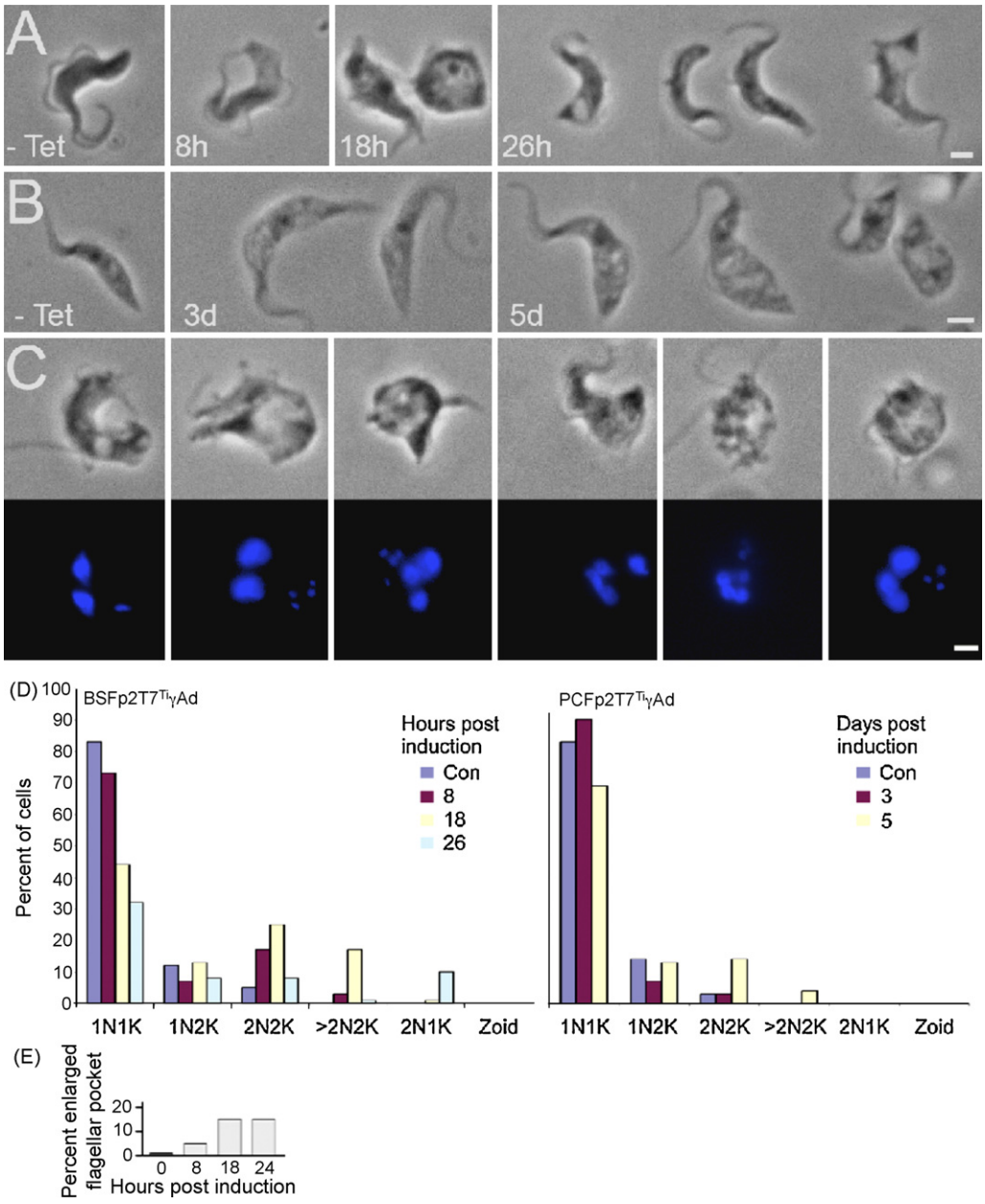


Fig. 5. Morphology and cell cycle progression of TbγAd knockdown cells. Morphology was monitored by phase contrast microscopy. (Panels A and B) Phase contrast galleries of a representative selection of BSF TbγAd RNAi cells (A) and PCF TbγAd RNAi cells (B), induced with 1 μg ml$^{-1}$ tetracycline for the indicated times (h = hours, d = days). Scale bar for both panels 2 μm. (Panel C) TbγAd RNAi causes nuclear segregation defects in BSF cells. Gallery of images cultures of BSFp2T7$^{Ti}$Ad cells induced for 26 h with 1 μg ml$^{-1}$ tetracycline showing a range of abnormalities in both phase morphology (top row) and DAPI stained DNA content (bottom row). Scale bar: 2 μm. (Panel D) Knockdown of TbγAd by RNAi blocks cytokinesis. BSF and PCF TbγAd RNAi cells were induced with 1 μg ml$^{-1}$ tetracycline for the indicated times, then fixed and stained with DAPI. The nucleus (N)/kinetoplast (K) ratios were determined for at least 100 cells at each time point. >2N:2K includes all cells with greater than two nuclei, "zoid" is a cell lacking a nucleus (cytoplast). (Panel E) Quantitation of kinetics of appearance of cells with and enlarged flagellar pocket in BSF TbγAd RNAi cells. BSFp2T7$^{Ti}$γAd cells were induced with 1 μg ml$^{-1}$ tetracycline for the indicated times, fixed with 4% paraformaldehyde and then adhered to slides. One hundred cells were analysed by phase contrast light microscopy for each time point to determine the percentage of cells with an enlarged pocket.

or TbEpsinR, the trypanosome epsin-related protein, do not result in mislocalisation of p67 [9] (Gabernet-Castello and MCF, unpublished data). As TbCLH RNAi provides a potent inhibition of endocytosis, this evidence effectively rules out a strict requirement for p67 trafficking *via* the plasma membrane.

Concerning AP-1 function, AP-1 is essential in both trypanosome major proliferative life stages, and the complex is constitutively expressed. Secondly, we demonstrate a clear relationship between the previously described β-subunit [11] and the γ-subunit, indicating they constitute the heavy chains of the trypanosome AP-1 complex. Thirdly, evidence suggests that AP-1 is not required for p67 lysosomal targeting or for VSG exocytosis. Fourthly, AP-1 is required for maintenance of the normal architecture of the endosomal system and for progres-

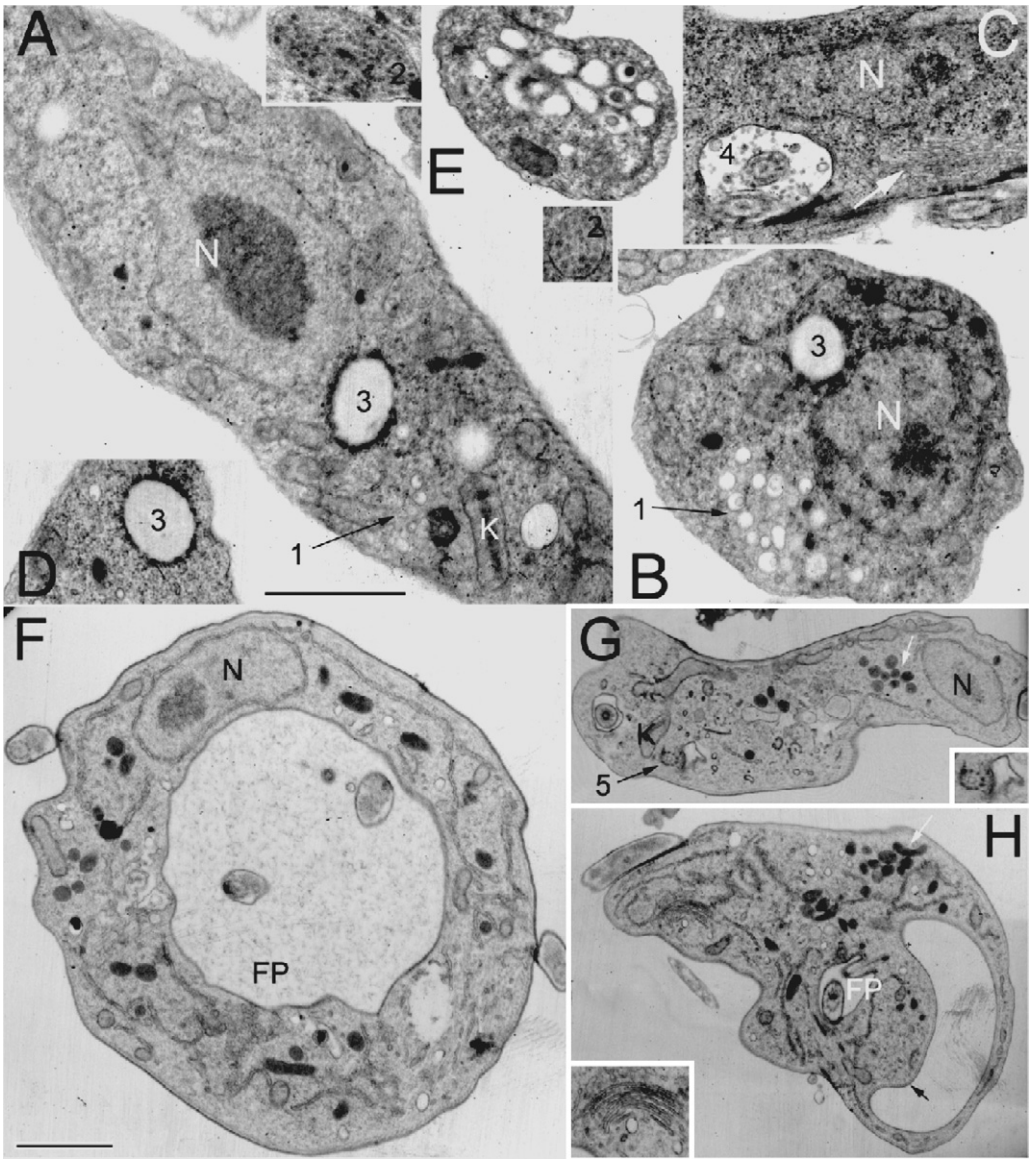


Fig. 6. Ultrastructural analysis of TbγAd knockdown cells. (Panels A–E) Electron micrographs of PCF cells following 3-day induction of TbγAd dsRNA. Note the abundance of large vesicles (1, arrow in panels B and E), prominent multivesicular bodies (2, insets in panel A), large vesicular structure surrounded by electron dense material (3 in panels A, B and D) and the inclusions in the flagellar pocket (4 in panel C). The Golgi complex profile is normal in these cells (panel C, white arrow). Scale bar on main image (A) 0.5 μm. (Panels F–H) Electron micrographs of BSF cells following 16 h induction of TbγAd dsRNA. The major morphological affect is an accumulation of electron dense vesicles in the cytoplasm (white arrows). There are also abnormalities in flagellar biosynthesis (note flagellum structure in the cytoplasm enlarged in the inset, 5, arrow in panel G) and plasma membrane invaginations (black arrow, panel H; note the presence of the microtubule corset beneath the membrane). The Golgi complex profile is normal (enlarged in the inset box in bottom right panel). Scale bar on main image (F) 0.5 μm. FP, flagellar pocket; N, nucleus; K, kinetoplast; G, Golgi.

sion through the cell cycle. The lack of a clear influence of AP-1 knockdown on p67 targeting was unexpected. AP-1 is constitutively expressed, and considering the absence of several additional trafficking factors from the trypanosome genome, we anticipated a major role for AP-1 in endosomal trafficking. The most probable explanations are either redundancy or that other AP complexes may substitute for AP-1 under conditions of the knockdown. The effects on endosome architecture and cell division likely explain the impact of AP-1 knockdown on viability but these defects are likely to be due to protracted disruption of trafficking pathways resulting in accumulation of mistargeted factors that cannot be tolerated. In essence these are secondary effects, notwithstanding a clear requirement for AP-1 expression for continued survival of the parasite. However, it remains formally possible that residual AP-1 expression in knockdown cells is sufficient to support p67 trafficking, but not continued cellular viability.

In mammalian cells it is AP-2 RNAi that leads to defective LAMP glycoprotein lysosomal targeting, with a considerable LAMP presence on the cell surface, but AP-2 is absent from *T. brucei* and other data argue against surface p67 trafficking. Knockdowns of AP-1, -3 or -4 components in mammalian cells have little effect on steady state LAMP targeting and there remains a considerable level of LAMP glycoprotein within the

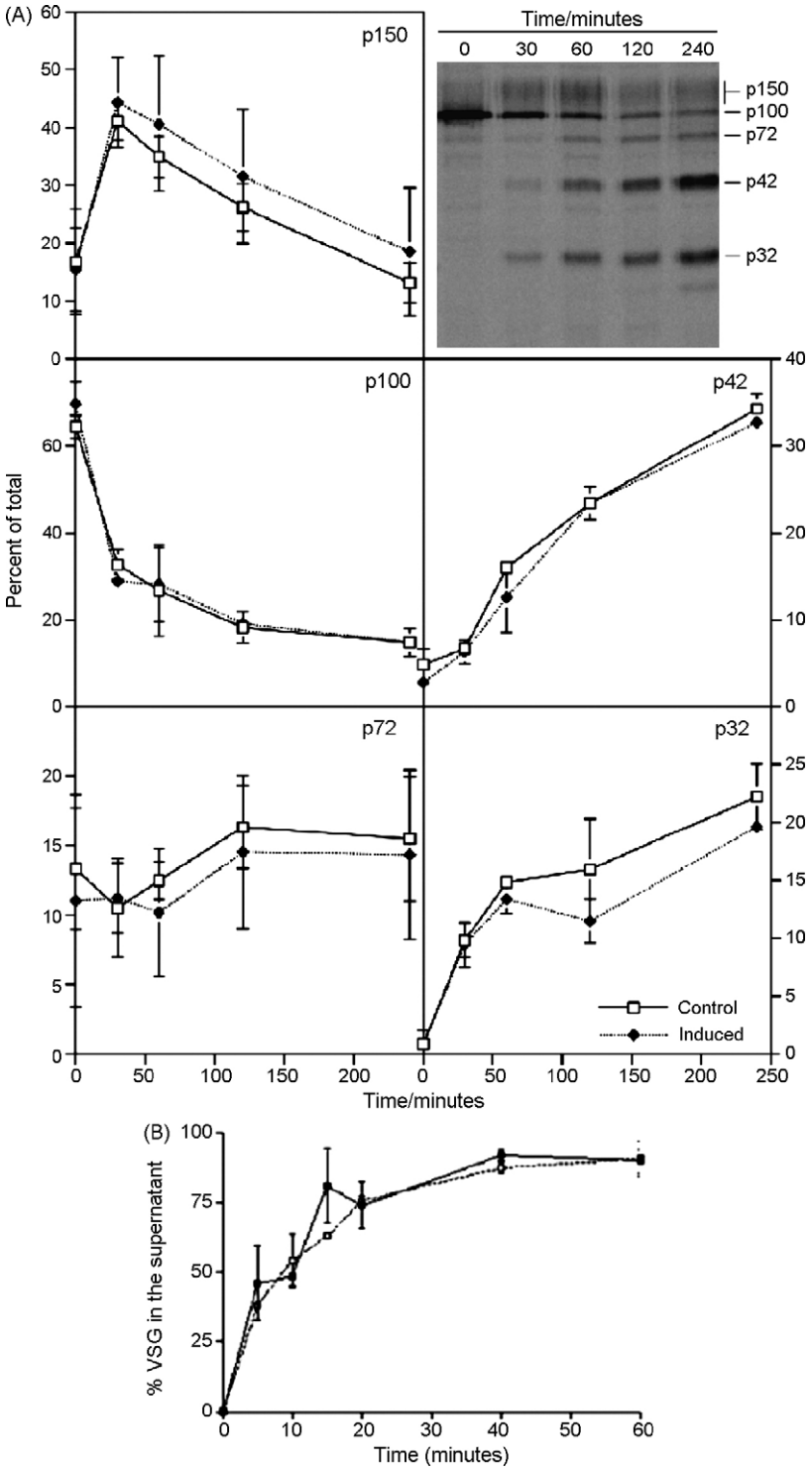


Fig. 7. TbγAd is not required for trafficking of newly synthesized VSG or p67 proteolytic processing. (Panel A) p67 processing is not significantly disrupted by TbγAd silencing. Following 18 h culturing in the absence (closed squares) or presence (open squares) of 1 μg ml$^{-1}$ tetracycline, BSFp2T7$^{Ti}$γAd cells were pulse-labelled with [$^{35}$S] methionine, followed by a chase period of up to 4 h. Cells were lysed and p67 was immunoprecipitated with mAb280. The different molecular weight proteolytic fragments produced during p67 processing in different intracellular compartments were separated by SDS-PAGE (data not shown) and the band intensities of the gp150, gp100, gp72, gp42 and gp32 fragments were quantified by denisitometry. Results are presented as percentage of the total recovered at each time point and are the mean from two experiments together with the standard error. Top right panel shows an example of a pulse-chase experiment to illustrate the sequential processing. (Panel B) Pulse-chase kinetic analysis of arrival of newly synthesized VSG at the plasma membrane. VSG export in uninduced (closed squares) and 18 h induced (open squares) BSFp2T7$^{Ti}$γAd cells was monitored by recovering soluble VSG (following hydrolysis from the plasma membrane by GPI-specific phospholipase C) from hypotonic lysates taken at the indicated time points following pulse labelling with [$^{35}$S]-methionine. Pulse labelled soluble VSG recovered following purification with Con-A sepharose was SDS-PAGE separated and quantified by densitometry. Data show the mean of two experiments with error bars indicating the standard error. Results are presented as percentages of the total recovered VSG in the supernatant, following background subtraction.

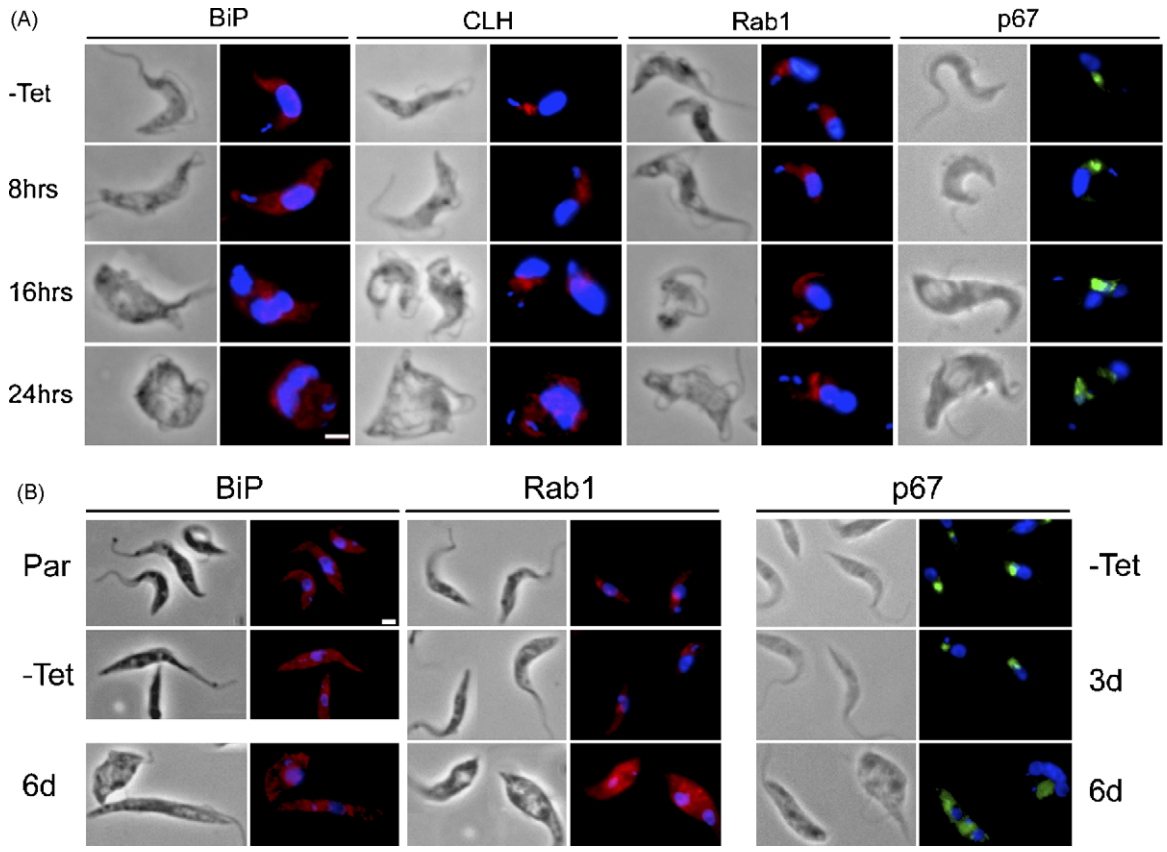


Fig. 8. TbγAd silencing does not cause mistargeting of p67. Immunofluorescence analysis for locations of lysosomal (p67), endoplasmic reticulum (TbBiP), Golgi complex (TbRAB1) and clathrin (TbCLH) proteins in BSF (panel A) or PCF (panel B) TbγAd RNAi cells. For each panel, left is phase, right is DAPI (DNA) in blue with p67 in green, or TbBiP, TbRAB1 or TbCLH in red. Induction times in 1 μg ml$^{-1}$ tetracycline are shown on the left of the images, or right for panel B, p67 data. Par = the parental PCF 29-13 cell line; −Tet = uninduced PCF or BSF TbγAd RNAi line. Scale bars: 2 μm.

lysosome, *albeit* with the possibility of an undetected kinetic transport defect [29]. We analysed in some detail the kinetics of p67 processing and it is unlikely that a simple kinetic effect can explain our observations. AP-1 RNAi may lead to activation of a compensatory pathway, as is observed for tyrosinase in mammalian cells where knockdown of one AP complex likely promotes interaction with other pathways [30]. Given cross recognition of dileucine signals by AP complexes, the potential for such behavior is present and likely explains the mild trafficking defects that are frequently observed for specific substrates versus the more severe general effects in other systems. Direct analysis of the AP-3 and -4 pathway, in combination with AP-1 knockdown, are required to determine if p67 is trafficked by these alternate pathways.

The trypanosome AP-1 knockdown phenotype is complex, including accumulation of cells post S-phase and/or with an enlarged flagellar pocket [9]. Both slow onset and low frequency of the phenotypes imply a secondary defect and a lack of mislocalisation of clathrin in the knockdown cells is consistent with this conclusion. Therefore AP-1 knockdown leads to accumulation of vesicular structures, most likely derived from post-Golgi compartments, and partly parallels similar experiments in higher eukaryotes [31,32]. AP-1 knockdowns/knockouts generate embryonic lethal phenotypes in *Mus musculis* [43] and *Caenorhabditis elegans*, suggesting essential developmental roles [33], However, in metazoan cell culture AP-1 is not required for cellular viability [41]. A mild phenotype is obtained by knockout of AP-1 components in *Saccharomyces cerevisiae*, and a potent trafficking defect is only apparent in combination with a *ts* clathrin heavy chain mutation [34]. In *Schizosaccharomyces pombe* the μ1 subunit is nonessential but cells accumulate cytoplasmic vacuoles [35]. In *Toxoplasma gondi* AP-1 knockdown leads to accumulation of vesicles, as well as engorgement of Golgi complex cisternae and impaired growth [36], while *Dictyostelium* AP-1 mutants produce a severe phenotype, including decreased growth, accumulation of cytosolic vesicles and defects in lysosomal enzyme sorting, but retain correct localisation of the majority of subcellular markers [32]. In *Leishmania*, the closest system to *T. brucei* so far analysed, AP-1 is not required for cell proliferation in culture but is required for infectivity and this difference between trypanosomes and *Leishmania* is highly intriguing [37]. Absence of the GGA proteins, down-regulated expression of the AP-3 complex in the bloodstream stage and absence of an AP-2 complex may explain essentiality in *T. brucei* as *Leishmania* retains AP-2. *Dictyostelium* and *T. gondii* both lack GGAs [1], consistent with GGA/AP-1 redundancy in mammals and yeast. This must however be offset against the lack of an effect on clathrin targeting; hence despite the essentiality of AP-1 in trypanosomes, there must be additional factors that are able to efficiently target

clathrin to endomembranes, and these could include AP-3, AP-4 or TbEpsinR. Further work is required to determine if this is indeed the case.

## Acknowledgements

This work was supported by a program grant from the Wellcome Trust (to MCF) and also the Sichuan Academy of Sciences (to DL). We thank James Bangs (Madison) and Keith Gull (Oxford) for generous provision of antibodies and David Goulding (London) for EM.

## Appendix A. Supplementary data

Supplementary data associated with this article can be found, in the online version, at doi:10.1016/j.molbiopara.2007.07.020.

## References

[1] Field MC, Gabernet-Castello C, Dacks JB. Reconstructing the evolution of the endocytic system: insights from genomics and molecular cell biology. In: Jékely G, editor. Origins and evolution of eukaryotic endomembranes and cytoskeleton. Eurekah/Landes Bioscience Press; 2006.
[2] Owen DJ, Collins BM, Evans PR. Adaptors for clathrin coats: structure and function. Annu Rev Cell Dev Biol 2004;20:153–91.
[3] Robinson MS. Adaptable adaptors for coated vesicles. Trends Cell Biol 2004;14:167–74.
[4] Eskelinen EL, Tanaka Y, Saftig P. At the acidic edge: emerging functions for lysosomal membrane proteins. Trends Cell Biol 2003;13(3):137–45.
[5] Rous BA, Reaves BJ, Ihrke G, et al. Role of adaptor complex AP-3 in targeting wild-type and mutated CD63 to lysosomes. Mol Biol Cell 2002;13(3):1071–82.
[6] Meyer C, Zizioli D, Lausmann S, et al. mu1A-adaptin-deficient mice: lethality, loss of AP-1 binding and rerouting of mannose 6-phosphate receptors. EMBO J 2000;19(10):2193–203.
[7] Kelley RJ, Brickman MJ, Balber AE. Processing and transport of a lysosomal membrane glycoprotein is developmentally regulated in African trypanosomes. Mol Biochem Parasitol 1995;74(2):167–78.
[8] Sheader K, Vaughan S, Minchin J, Hughes K, Gull K, Rudenko G. Variant surface glycoprotein RNA interference triggers a precytokinesis cell cycle arrest in African trypanosomes. Proc Natl Acad Sci USA 2005;102:8716–21.
[9] Allen CL, Goulding D, Field MC. Clathrin-mediated endocytosis is essential in *Trypanosoma brucei*. EMBO J 2003;22:4991–5002.
[10] Jeffries TR, Morgan GW, Field MC. A developmentally regulated rab11 homologue in *Trypanosoma brucei* is involved in recycling processes. J Cell Sci 2001;114(Pt 14):2617–26.
[11] Morgan GW, Allen CL, Jeffries TR, Hollinshead M, Field MC. Developmental and morphological regulation of clathrin-mediated endocytosis in *Trypanosoma brucei*. J Cell Sci 2001;114:2605–15.
[12] Berriman M, Ghedin E, Hertz-Fowler C, et al. The genome of the African trypanosome *Trypanosoma brucei*. Science 2005;309:416–22.
[13] Qiao X, Chuang BF, Jin Y, et al. Sorting signals required for trafficking of the cysteine-rich acidic repetitive transmembrane protein in *Trypanosoma brucei*. Eukaryot Cell 2006;5(8):1229–42.
[14] LaCount DJ, Bruse S, Hill KL, Donelson JE. Double-stranded RNA interference in *Trypanosoma brucei* using head-to-head promoters. Mol Biochem Parasitol 2000;111:67–76.
[15] Redmond S, Vadivelu J, Field MC. RNAit: an automated web-based tool for the selection of RNAi targets in *Trypanosoma brucei*. Mol Biochem Parasitol 2003;128:115–8.
[16] Bangs JD, Uyetake L, Brickman MJ, Balber AE, Boothroyd JC. Molecular cloning and cellular localization of a BiP homologue in *Trypanosoma brucei*. Divergent ER retention signals in a lower eukaryote. J Cell Sci 1993;105:1101–13.
[17] Alexander DL, Schwartz KJ, Balber AE, Bangs JD. Developmentally regulated trafficking of the lysosomal membrane protein p67 in *Trypanosoma brucei*. J Cell Sci 2002;115:3253–63.
[18] Dhir V, Goulding D, Field MC. TbRAB1 and TbRAB2 mediate trafficking through the early secretory pathway of *Trypanosoma brucei*. Mol Biochem Parasitol 2004;137:253–65.
[19] Hall BS, Pal A, Goulding D, Field MC. Rab4 is an essential regulator of lysosomal trafficking in trypanosomes. J Biol Chem 2004;279:45047–56.
[20] Hall B, Allen CL, Goulding D, Field MC. Both of the Rab5 subfamily small GTPases of *Trypanosoma brucei* are essential and required for endocytosis. Mol Biochem Parasitol 2004;138:67–77.
[21] Chung WL, Carrington M, Field MC. Cytoplasmic targeting signals in transmembrane invariant surface glycoproteins of trypanosomes. J Biol Chem 2004;279(52):54887–95.
[22] Peden AA, Rudge RE, Lui WW, Robinson MS. Assembly and function of AP-3 complexes in cells expressing mutant subunits. J Cell Biol 2002;156:327–36.
[23] Williams RA, Tetley L, Mottram JC, Coombs GH. Cysteine peptidases CPA and CPB are vital for autophagy and differentiation in *Leishmania mexicana*. Mol Microbiol 2006;61(3):655–74.
[24] Hall BS, Smith E, Langer W, Jacobs LA, Goulding D, Field MC. Developmental variation in Rab11-dependent trafficking in *Trypanosoma brucei*. Eukaryot Cell 2005;4:971–80.
[25] Hall BS, Pal A, Goulding D, Acosta-Serrano A, Field MC. *Trypanosoma brucei*: TbRAB4 regulates membrane recycling and expression of surface proteins in procyclic forms. Exp Parasitol 2005;111:160–71.
[26] Grunfelder CG, Engstler M, Weise F, et al. Endocytosis of a glycosylphosphatidylinositol-anchored protein via clathrin-coated vesicles, sorting by default in endosomes, and exocytosis via RAB11-positive carriers. Mol Biol Cell 2003;14:2029–40.
[27] Voorhees P, Deignan E, van Donselaar E, et al. An acidic sequence within the cytoplasmic domain of furin functions as a determinant of *trans*-Golgi network localization and internalization from the cell surface. EMBO J 1995;14:4961–75.
[28] Kyttala A, Yliannala K, Schu P, Jalanko A, Luzio JP. AP-1 and AP-3 facilitate lysosomal targeting of Batten disease protein CLN3 via its dileucine motif. J Biol Chem 2005;280(11):10277–83.
[29] Janvier K, Bonifacino JS. Role of the endocytic machinery in the sorting of lysosome-associated membrane proteins. Mol Biol Cell 2005;16(9):4231–42. Epub June 29, 2005.
[30] Theos AC, Tenza D, Martina JA, et al. Functions of AP-3 and AP-1 in tyrosinase sorting from endosomes to melanosomes. Mol Biol Cell 2005;16:5356–72.
[31] Hirst J, Miller SE, Taylor MJ, von Mollard GF, Robinson MS. EpsinR is an adaptor for the SNARE protein Vti1b. Mol Biol Cell 2004;15:5593–602.
[32] Lefkir Y, de Chassey B, Dubois A, et al. The AP-1 clathrin-adaptor is required for lysosomal enzymes sorting and biogenesis of the contractile vacuole complex in *Dictyostelium* cells. Mol Biol Cell 2003;14:1835–51.
[33] Shim J, Sternberg PW, Lee J. Distinct and redundant functions of μ1 medium chains of the AP-1 clathrin-associated protein complex in the nematode *Caenorhabditis elegans*. Mol Biol Cell 2000;11:2743–56.
[34] Rad MR, Phan HL, Kirchrath L, et al. *Saccharomyces cerevisiae* Apl2p, a homologue of the mammalian clathrin AP beta subunit, plays a role in clathrin-dependent Golgi functions. J Cell Sci 1995;108:1605–15.
[35] Kita A, Sugiura R, Shoji H, et al. Loss of Apm1, the μ1 subunit of the clathrin-associated adaptor–protein-1 complex, causes distinct phenotypes and synthetic lethality with calcineurin deletion in fission yeast. Mol Biol Cell 2004;15:2920–31.
[36] Ngo HM, Yang M, Paprotka K, Pypaert M, Hoppe H, Joiner KA. AP-1 in *Toxoplasma gondii* mediates biogenesis of the rhoptry secretory organelle from a post-Golgi compartment. J Biol Chem 2003;278:5343–52.
[37] Gokool S. σ1- and μ1-Adaptin homologues of *Leishmania mexicana* are required for parasite survival in the infected host. J Biol Chem 2003;278(32):29400–9.

[38] Brickman MJ, Balber AE. Transport of a lysosomal membrane glycoprotein from the Golgi to endosomes and lysosomes via the cell surface in African trypanosomes. J Cell Sci 1994;107(Pt 11):3191–200.

[39] Bangs JD, Brouch EM, Ransom DM, Roggy JL. A soluble secretory reporter system in Trypanosoma brucei. Studies on endoplasmic reticulum targeting J Biol Chem 1996;271(31):18387–93.

[40] Bonifacino JS, Traub LM. Signals for sorting of transmembrane proteins to endosomes and lysosomes. Annu Rev Biochem 2003;72:395–447.

[41] Hirst J, Lindsay MR, Robinson MS. GGAs: roles of the different domains and comparison with AP-1 and clathrin. Mol Biol Cell 2001;12(11):3573–88.

[42] Adl SM, Simpson AG, Farmer MA, et al. The new higher level classification of eukaryotes with emphasis on the taxonomy of protists. J Eukaryot Microbiol 2005;52(5):399–451.

[43] Zizioli D, Meyer C, Guhde G, Saftig P, von Figura K, Schu P. Early embryonic death of mice deficient in gamma-adaptin. J Biol Chem 1999;274(9):5385–90.